CAMBRIDGE
UNIVERSITY PRESS

Article

From structure topology to chemical composition. XXVI. Crystal structure and chemical composition of a possible new mineral of the murmanite group (seidozerite supergroup), ideally Na₂CaTi₄(Si₂O₇)₂O₄(H₂O)₄, from the Lovozero alkaline massif, Kola Peninsula, Russia

Elena Sokolova* and Frank C. Hawthorne

Department of Geological Sciences, University of Manitoba, 125 Dysart Road, Winnipeg, MB, R3T 2N2 Canada

Abstract

The crystal structure of a murmanite-related mineral (MRM) of the murmanite group (seidozerite supergroup), ideally $Na_2CaTi_4(Si_2O_7)_2O_4(H_2O)_4$, from Mt. Pyalkimpor, the Lovozero alkaline massif, Kola Peninsula, Russia, was refined in space group $P\bar{1}$ with $a = 5.363(2)$, $b = 7.071(2)$, $c = 12.176(5)$ Å, $\alpha = 92.724(3)$, $\beta = 107.542(7)$, $\gamma = 90.13(2)°$, $V = 439.7(4)$ Å³ and $R_1 = 5.72\%$. On the basis of electron-microprobe analysis, the empirical formula calculated on 22 (O + F), with two constraints derived from structure refinement, OH = 0.11 per formula unit (pfu) and H_2O = 3.89 pfu, is $(Na_{2.12}K_{0.07}Sr_{0.01})_{\Sigma2.20}Ca_{0.85}(Ti_{3.01}Nb_{0.39}Mn_{0.20}Fe^{2+}_{0.19}Mg_{0.17}Zr_{0.01}Al_{0.01})_{\Sigma3.98}(Si_{4.20}O_{14})[O_{3.90}F_{0.10}]_{\Sigma4}[(H_2O)_{3.89}(OH)_{0.11}]_{\Sigma4}\{P_{0.03}\}$, with $Z = 1$. It seems unlikely that $\{P_{0.03}\}$ belongs to MRM itself. The crystal structure of MRM is an array of TS blocks (Titanium-Silicate) connected via hydrogen bonds. The TS block consists of HOH sheets (H = heteropolyhedral, O = octahedral) parallel to (001). In the O sheet, the Ti-dominant M^O1 site and Ca-dominant M^O2 site give ideally $(Ca\square)Ti_2$ pfu. In the H sheet, the Ti-dominant M^H site and Na-dominant A^P site give ideally Na_2Ti_2 pfu. The M^H and A^P polyhedra and Si_2O_7 groups constitute the H sheet. The ideal structural formula of MRM of the form $A^P_2M^H_2M^O_4(Si_2O_7)_2(X^O_{M,A})_4(X^P_A)_2(X^P_{M,A})_4$ is $Na_2Ti_2(Ca\square)Ti_2(Si_2O_7)_2O_4(H_2O)_4$. MRM is a Ca-rich and Na-poor analogue of murmanite, ideally $Na_2Ti_2Na_2Ti_2(Si_2O_7)_2O_4(H_2O)_4$ and a Na-rich and (OH)-poor analogue of calciomurmanite, ideally $(Ca\square)Ti_2(Na\square)Ti_2(Si_2O_7)_2O_2[O(OH)](H_2O)_4$. MRM and (murmanite and calciomurmanite) are related by the following substitutions: $^O(Ca^{2+}\square)_{MRM} \leftrightarrow {}^O(Na_2^+)_{mur}$ and $^O(Ca^{2+}\square)_{MRM} + {}^H(Na_2^+)_{MRM} + {}^O(O^{2-})_{MRM} \leftrightarrow {}^O(Na^+\square)_{cal} + {}^H(Ca^{2+}\square)_{cal} + {}^O[(OH)^-]_{cal}$. MRM is a possible new mineral of the murmanite group (seidozerite supergroup) where Ti + Mn + Mg = 4 apfu.

Keywords: murmanite-related mineral, crystal structure, electron microprobe analysis, chemical formula, TS block, murmanite group, seidozerite supergroup

(Received 14 January 2018; accepted 27 February 2018)

Introduction

Lykova *et al.* (2016) published the description of calciomurmanite, $(Na,\square)_2Ca(Ti,Mg,Nb)_4[Si_2O_7]_2O_2(OH,O)_2(H_2O)_4$, a new mineral from the Lovozero and Khibiny alkaline massifs, Kola Peninsula, Russia. They described calciomurmanite as a Na–Ca ordered analogue of murmanite and related calciomurmanite to two murmanite-group minerals: murmanite, ideally $Na_4Ti_4(Si_2O_7)_2O_4(H_2O)_4$ (Gutkova, 1930; Cámara *et al.*, 2008) (Table 1) and kolskyite, ideally $Na_2CaTi_4(Si_2O_7)_2O_4(H_2O)_7$ (Cámara *et al.*, 2013a). Table 1 lists selected murmanite-group minerals with the structure type B1MG. In accord with

Sokolova and Cámara (2013), B1 = Basic structure type 1 and MG = murmanite group. Lykova *et al.* (2016) reported the chemical composition of calciomurmanite from three localities: (1) Mt. Flora, Lovozero (holotype, V.I. Stepanov collection, Fersman Mineralogical Museum, Moscow, Russia); (2) Mt. Eveslochorr, Khibiny (cotype, collection of the Bel'kov Museum of Geology and Mineralogy; Geological Institute, Apatity, Russia) and (3) the Shcherbakovitovoe pegmatite, Mt. Koashva, Khibiny (found by I.V. Pekov in 2008) [see chemical analyses for localities (1) and (3) in Table 2], the empirical formula $Na_{1.34}Ca_{1.04}K_{0.05}Mg_{0.49}Mn_{0.29}Fe^{2+}_{0.21}Nb_{0.36}Ti_{2.85}(Si_{3.87}Al_{0.13})_{\Sigma4}O_{16.40}(OH)_{1.6}(PO_4)_{0.03}(H_2O)_{4.94}$ (holotype) with $Z = 1$ (Table 2) and its crystal structure ($R_1 = 6.56$ and 6.63% for holotype and cotype, respectively). Lykova *et al.* (2016) outlined the main features of the structural relation between calciomurmanite and murmanite: (1) the H sheet: in calciomurmanite (holotype and cotype), the $^{[8]}A^P$ site is occupied by Ca at 58 and 50%; in murmanite, the $^{[8]}A^P$ site is occupied by Na; (2) the O sheet: in calciomurmanite, the $^{[6]}M^O2$ site is occupied by Na at 71 and 52%; in murmanite, the $^{[6]}M^O2$ site is occupied

*Author for correspondence: Elena Sokolova, email: elena_sokolova@umanitoba.ca

Associate Editor: Ed Grew

Table 1. Ideal structural formulae and crystallographic information for selected murmanite-group minerals* (seidozerite supergroup), Ti = 4 apfu.

Mineral	Ideal structural formula								a (Å)	b (Å)	c (Å)	α (°)	β (°)	γ (°)	Space group	Z	Ref.[†]
	A_2^P	M_2^H	$(M^O1)_2$	$(M^O2)_2$	$(Si_2O_7)_2$	$(X_M^O)_2$	$(X_A^O)_2$	$(X_{M,A}^P)_4$									
Murmanite**	$^{[8]}Na_2$	Ti_2	Ti_2	Na_2	$(Si_2O_7)_2$	O_2	O_2	$(H_2O)_4$	5.388	7.058	12.176	93.51	107.94	90.09	$P\bar{1}$	1	(1,2)
									5.388	7.058	11.699	93.76		98.04	89.91			
Murmanite-related mineral (MRM)	$^{[8]}Na_2$	Ti_2	Ti_2	$(Ca\square)$	$(Si_2O_7)_2$	O_2	O_2	$(H_2O)_4$	5.363	7.071	12.176	92.72	107.54	90.13	$P\bar{1}$	1	(–,3)
Calciomurmanite	$(^{[8]}Ca\square)$	Ti_2	Ti_2	$(Na\square)$	$(Si_2O_7)_2$	O_2	$[O(OH)]$	$(H_2O)_4$	5.347	7.077	12.146	91.83	107.53	90.16	$P\bar{1}$	1	(4,4)
Vigrishinite	$Zn\square$	Ti_2	Ti_2	$Na\square$	$(Si_2O_7)_2$	O_2	$O(OH)$	$(H_2O)_4$	10.530	13.833	11.659	94.34	98.30	89.80	$C\bar{1}$	4	(5,6)

*Ideal structural formulae are from Sokolova and Cámara (2017); unit-cell parameters are given to the third decimal. Labelling is in accord with Sokolova (2006): M_4^O and M_2^H = cations of the O and H sheets, and A_2^P = cations at the peripheral (P) sites; $(X_{M,A}^O)_4$ = anions of the O sheet not bonded to Si; $(X_M^O)_2$ = anions at the apical vertices of 3M^O polyhedra; $(X_A^O)_2$ = anions at the common vertices of 3M^O and A^P polyhedra; X_M^P and X_A^P = apical anions of M^H and A^P cations at the periphery of the TS block; and coordination numbers are given for non-octahedrally coordinated cation sites;

**for murmanite, unit cells [1, upper line] → [2, lower line] are related by the transformation matrix (100/0$\bar{1}$0/$\bar{1}$0$\bar{1}$);

†First reference: the discovery of the mineral; second: the most recent reference on the structure: (1) Gutkova *et al.* (1930); (2) Cámara *et al.* (2008); (3) this work; (4) Lykova *et al.* (2016); (5) Pekov *et al.* (2013); (6) Sokolova and Hawthorne (2018).

Table 2. Chemical composition and unit formula for MRM.

Chemical composition (wt.%)					Unit formula* (apfu)				
	MRM (1)	Calciomurmanite (2)	(3)	Murmanite (4)		MRM (1)	Calciomurmanite (2)	(3)	Murmanite (4)
Nb_2O_5	6.56	10.94	6.14	8.32	Nb	0.39	0.67	0.36	0.51
P_2O_5	0.23	1.12	0.27	n.d.	P	0.03	0.13	0.03	
ZrO_2	0.14	n.d.	n.d.	0.14	Zr	0.01			0.01
TiO_2	30.47	27.49	29.69	29.92	Ti	3.01	2.79	2.85	3.08
SiO_2	31.96	29.65	30.27	28.92	Si	4.20	4.00	3.87	3.96
Al_2O_3	0.08	0.06	0.85	n.d.	Al	0.01	0.00	0.13	
Fe_2O_3	n.a.	n.a.	n.a.	1.46**	Fe^{3+}				0.15
SrO	0.09	n.d.	n.d.	n.d.	Sr	0.01			
FeO	1.70	1.77	1.93	0.00	Fe^{2+}	0.19	0.20	0.21	
MnO	1.77	2.90	2.65	2.83	Mn	0.20	0.33	0.29	0.33
CaO	6.02	6.90	7.61	1.43	Ca	0.85	1.00	1.04	0.21
MgO	0.85	0.22	2.54	0.35	Mg	0.17	0.04	0.49	0.07
K_2O	0.43	0.64	0.30	0.28	K	0.07	0.11	0.05	0.05
Na_2O	8.32	8.87	5.39	12.52	Na	2.12	2.32	1.34	3.32
F	0.23	n.a.	n.a.	0.56	Σcations	11.25	11.59	10.66	11.69
H_2O	9.00***	n.a.	11.59†	8.77***					
O = F	−0.10			−0.24	F	0.10			0.24
Total	97.75	90.56	99.23	95.26	H^+	7.89		11.18	8.00
					OH	0.11		1.60	
					H_2O	3.89		4.94	4.00
					Σ(anions, H_2O gr.)	22.00		23.06	22.00

(1) This work, Mt. Pyalkimpor, Lovozero; (2 and 3) are taken from Lykova *et al.* (2016): (2) Shcherbakovitovoe pegmatite, Mt. Koashva, Khibiny; (3) Mt. Flora, Lovozero (holotype); and (4) after Cámara *et al.* (2008): Yubileynaya pegmatite, Mt. Karnasurt, Lovozero. 4.2% of lomonosovite intergrowth was subtracted.

n.a. = not analysed; n.d. = not detected; structure work done for (1,3,4).

*Formulae calculated on: (1) 22 (O + F) apfu, with OH = 0.11 pfu and H_2O = 3.89 pfu and (2, 3) Si + Al = 4 apfu and OH⁻/O²⁻ ratio calculated by charge balance; and (4) 22 (O + F) apfu, with H_2O = 4 pfu.

**Determined by Mössbauer spectroscopy.

***Calculated from crystal-structure refinement.

†Measured by the modified Penfield method (Lykova *et al.*, 2016).

by Na. Taking into account the structural information of Lykova *et al.* (2016) and the content of 1.34 Na and 1.04 Ca apfu (atoms per formula unit) in the empirical formula (see above), Sokolova and Cámara (2017) wrote the ideal structural formula of calciomurmanite of the form $A_2^P M_2^H M_4^O (Si_2O_7)_2 (X_M^O)_2 (X_A^O)_2 (X_{M,A}^P)_4$ as $(Ca\square)Ti_2(Na\square)Ti_2(Si_2O_7)_2O_2[O(OH)](H_2O)_4$ [Table 1, site labelling is in accord with Sokolova (2006)].

Following our previous work on murmanite, ideally $Na_4Ti_4(Si_2O_7)_2O_4(H_2O)_4$ (Cámara *et al.*, 2008) and a murmanite-related mineral vigrishinite, ideally $NaZnTi_4(Si_2O_7)_2O_3(OH)(H_2O)_4$ (Sokolova and Hawthorne, 2018), we wanted to understand

the details of the bond topology in the structure of calciomurmanite, especially the pattern of hydrogen bonding. In February of 2017 at the Tucson Gem and Mineral Show, we purchased a 'calcio-murmanite' sample from Mt. Pyalkimpor, the Lovozero alkaline massif, Kola Peninsula, Russia, from Dmitriy Belakovskiy. Dmitry told us that it was a new finding of 'calciomurmanite' by Inna Lykova in 2016, after the approval of calciomurmanite by the International Mineralogical Association Commission on New Minerals, Nomenclature and Classification (IMA2014-103, Lykova, 2015). Our work on the new 2016-finding of 'calciomur-manite' has resulted in chemical composition and stereochemistry

different from both calciomurmanite (holotype: Mt. Flora, Lovozero, and cotype: Mt. Eveslochorr, Khibiny) and murmanite. Here, we report the chemical composition and the refinement of the crystal structure of this murmanite-related mineral (MRM), a possible new mineral of the murmanite group, which we purchased under the name 'calciomurmanite'.

Description of the sample

MRM occurs as large platy grains up to 5 mm x 10 mm across and up to 1 mm thick. It is opaque in large grains and cleavage plates, very pale-brown in thick fragments, and colourless and transparent in very small thin plates.

Chemical analysis

The crystal of MRM used for the structure refinement was analysed with a Cameca SX-100 electron-microprobe operating in wavelength-dispersion mode with an accelerating voltage of 15 kV, a specimen current of 5 nA, a beam diameter of 10 μm and count times on peak and background of 20 and 10 s, respectively. The following standards were used: Si and Ca: diopside; Al: andalusite; F: fluoro-riebeckite; Na: albite; Nb: $Ba_2NaNb_5O_{15}$; Zr: zircon; Mg: forsterite, Fe: fayalite; Mn: spessartine; Sr: $SrTiO_3$; Ti: titanite; K: orthoclase; and P: apatite. Zinc and Ta were sought but not detected. Data were reduced using the φ(ρZ) procedure of Pouchou and Pichoir (1985). The chemical composition of MRM is the mean of four determinations and is given in Table 2, analysis (1). Our chemical analysis of MRM is close to that of 'calciomurmanite' from the Shcherbakovitovoe pegmatite, Mt. Koashva, Khibiny [Table 2, analysis (2), from Lykova *et al.*, 2016], particularly for the Na_2O content, 8.32 *vs.* 8.87 wt.%, and the Al_2O_3 content, 0.08 *vs.* 0.06 wt.%. Comparison of our chemical analysis and that of the holotype calciomurmanite from Mt. Flora, Lovozero (holotype) [Table 2, analysis (3), from Lykova *et al.*, 2016], shows differences in the Na_2O content, 8.32 *vs.* 5.39 wt.%, and the Al_2O_3 content, 0.08 *vs.* 0.85 wt.%. The analyses (1), (2) and (3) (Table 2) give the following values for the content of CaO: 6.02, 6.90 and 7.61 wt.%, respectively, and these three values are much higher than that for murmanite, 1.43 wt.% [Table 2, analysis (4), from Cámara *et al.*, 2008]. The empirical formula of MRM, calculated on the basis of 22 (O + F), with two constraints derived from the crystal-structure refinement, OH = 0.11 pfu and H_2O = 3.89 pfu, is $(Na_{2.12}K_{0.07}Sr_{0.01})_{\Sigma2.20}Ca_{0.85}(Ti_{3.01}Nb_{0.39}Mn_{0.20}Fe^{2+}_{0.19}Mg_{0.17}Zr_{0.01}Al_{0.01})_{\Sigma3.98}(Si_{4.20}O_{14})[O_{3.90}F_{0.10}]_{\Sigma4}[(H_2O)_{3.89}(OH)_{0.11}]_{\Sigma4}\{P_{0.03}\}$ with Z = 1. We suggest that $\{P_{0.03}\}$ belongs to other phases which form intergrowths with MRM. Intimate intergrowths are very common for TS-block minerals: our high-resolution transmission electron microscopy work on murmanite-group minerals lomonosovite, $Na_{10}Ti_4(Si_2O_7)_2(PO_4)_2O_4$, and betalomonosovite, $Na_6Ti_4(Si_2O_7)_2[PO_3(OH)][PO_2(OH)_2]O_3F$ (Sokolova *et al.*, 2015); zvyaginite, $Na_2ZnTiNb_2(Si_2O_7)_2O_2(OH)_2(H_2O)_4$, a lamprophyllite-group mineral (Sokolova *et al.*, 2017), and cámaraite, $NaBa_3Fe^{2+}_8Ti_4(Si_2O_7)_4O_4(OH)_4F_3$, a bafertisite-group mineral (Cámara *et al.*, 2009), shows that these four TS-block minerals contain intergrown phases.

X-ray data collection and structure refinement

X-ray data for the MRM single crystal were collected with a Bruker APEX II ULTRA three-circle diffractometer equipped

Table 3. Miscellaneous structure-refinement data for MRM.

Crystal data	
Ideal formula	$Na_2CaTi_4(Si_2O_7)_2O_4(H_2O)_4$
Crystal system, space group	triclinic, $P\bar{1}$
Temperature (K)	293(2)
a, b, c (Å)	5.363(2), 7.071(2), 12.176(5)
α, β, γ (°)	92.724(7), 107.542(7), 90.13(2)
V (Å³)	439.7(4)
Z	1
Absorption coefficient (mm⁻¹)	2.63
F(000)	380.0
$D_{calc.}$ (g/cm³)	2.919
Data collection	
Crystal description	Colourless transparent plate
Crystal size (mm)	0.100 x 0.050 x 0.004
Instrument	Bruker APEX II ULTRA
Radiation/monochromator	Mo*K*α/ graphite
2θ$_{max}$ (°)	60.16
Absorption correction	Empirical (*SADABS*, Sheldrick, 2008)
T_{min}, T_{max}	0.7858, 0.9281
No. of measured, independent and observed [F_o > 4σF] reflections	5143, 2579, 2254
R_{int} (%)	0.0264
Range of *h, k, l*	−7 ≤ h ≤ 7, −9 ≤ k ≤ 9, −17 ≤ l ≤ 17
Frame width (°), time (s)	0.5, 30
Refinement	
Refinement method	Full-matrix least squares on F^2, fixed weights proportional to $1/\sigma F_o^2$
Final R_{obs}	
R_1[F_o > 4σF], R_1(all)	0.0572, 0.0668
wR_2	0.1308
Goodness of fit on F^2	1.168
No. refined parameters	172
Δρ$_{max}$, Δρ$_{min}$ (e⁻ Å⁻³)	1.77, −0.89

with a rotating-anode generator (Mo*K*α radiation), multilayer optics and an APEX II 4K CCD detector. Details of data collection and structure refinement are given in Table 3. The intensities of reflections with −7 ≤ h ≤ 7, −9 ≤ k ≤ 9, −17 ≤ l ≤ 17 were collected with a frame width of 0.5° and a frame time of 30 s, and an empirical absorption correction (SADABS, Sheldrick, 2008) was applied. The crystal structure of MRM was refined using the coordinates of Cámara *et al.* (2008) for murmanite in space group $P\bar{1}$ to R_1 = 5.72% with the Bruker *SHELXTL* Version 5.1 (Sheldrick, 2015). There are six cation sites in the crystal structure of MRM: the M^H, A^P and two Si sites of the H sheet and two M^O sites of the O sheet; labelling follows Sokolova (2006). We encountered a split of the M^H site into two subsites, M^H1 and M^H2, 0.38 Å apart. For the refinement, we constrained atoms at those two subsites of the M^H site to have the same displacement parameters (using EADP constraints). The occupancies of five sites/subsites were refined with the following scattering curves: $M^H1,2$ and M^O1 sites: Ti; M^O2 site: Na; and A^P site: Ca. The coordinates of the H atoms were refined where the D (donor)–H distances were softly constrained to 0.98 Å. Scattering curves for neutral atoms were taken from the *International Tables for Crystallography* (Wilson, 1992). Final atom coordinates and equivalent displacement parameters are given in Table 4, selected interatomic distances and angles in Table 5, refined site-scattering values and assigned site-populations in Table 6, bond-valence values in Table 7 and details of hydrogen bonding in Table 8. A list of observed and calculated structure factors and a Crystallography Information File (CIF) have been deposited with the Principal Editor of *Mineralogical Magazine* and are available as Supplementary material (see below).

Table 4. Final atom coordinates and displacement parameters (Å^2) for MRM.

Atom	x	y	z	U^{11}	U^{22}	U^{33}	U^{23}	U^{13}	U^{12}	U_{eq}
M^H1	0.4164(5)	0.3271(2)	0.2403(6)	0.0052(4)	0.0087(4)	0.0184(18)	0.0037(5)	0.0058(7)	0.0013(3)	0.0102(6)
M^H2	0.393(3)	0.3317(19)	0.208(3)	0.0052(4)	0.0087(4)	0.0184(18)	0.0037(5)	0.0058(7)	0.0013(3)	0.0102(6)
M^O1	0.27292(16)	0.88353(11)	0.50532(7)	0.0158(4)	0.0137(4)	0.0174(4)	0.0028(3)	0.0036(3)	0.0032(3)	0.0159(3)
M^O2	0.7258(7)	0.6062(4)	0.4891(3)	0.041(2)	0.0231(17)	0.038(2)	0.0112(13)	0.0241(16)	0.0146(13)	0.0309(11)
A^P	0.3861(4)	0.8299(3)	0.20111(17)	0.0268(10)	0.0200(9)	0.0314(11)	0.0010(7)	0.0089(7)	0.0001(6)	0.0260(6)
Si1	0.9234(2)	0.05211(16)	0.26042(11)	0.0092(5)	0.0075(5)	0.0160(6)	0.0023(4)	0.0041(4)	−0.0004(4)	0.0108(3)
Si2	0.9462(2)	0.62319(17)	0.27710(11)	0.0124(6)	0.0080(5)	0.0178(6)	0.0019(4)	0.0049(5)	0.0012(4)	0.0126(3)
O1	0.1403(8)	0.1369(7)	0.2103(3)	0.026(2)	0.049(3)	0.0202(19)	−0.0001(17)	0.0097(16)	−0.0219(19)	0.0314(10)
O2	0.6394(8)	0.1324(6)	0.2020(3)	0.0213(19)	0.043(2)	0.023(2)	−0.0023(17)	0.0024(15)	0.0198(17)	0.0302(9)
O3	0.0022(6)	0.9323(5)	0.5988(3)	0.0132(14)	0.0152(15)	0.0163(16)	0.0042(12)	0.0047(12)	0.0017(12)	0.0147(6)
O4	0.9016(9)	0.8276(5)	0.2185(3)	0.045(2)	0.0093(15)	0.0232(19)	0.0020(13)	0.0063(17)	0.0019(15)	0.0267(9)
O5	0.6679(8)	0.5215(7)	0.2381(4)	0.026(2)	0.049(3)	0.036(2)	0.005(2)	0.0104(18)	−0.026(2)	0.0367(11)
O6	0.0530(8)	0.6632(5)	0.4158(3)	0.030(2)	0.0177(17)	0.0196(16)	0.0029(13)	0.0033(15)	0.0034(14)	0.0231(8)
O7	0.1637(8)	0.5221(7)	0.2322(4)	0.025(2)	0.044(3)	0.034(2)	0.0008(19)	0.0076(17)	0.0220(19)	0.0346(10)
X^O_M	0.5326(7)	0.2982(5)	0.3927(3)	0.0169(16)	0.0230(17)	0.0206(17)	0.0058(13)	0.0054(13)	0.0003(13)	0.0201(7)
X^O_A	0.5020(7)	0.8937(5)	0.4126(3)	0.0159(15)	0.0168(16)	0.0158(15)	0.0013(12)	0.0063(12)	−0.0004(12)	0.0159(7)
X^P_M	0.2809(10)	0.3453(7)	0.0460(4)	0.044(3)	0.034(2)	0.029(2)	0.0054(18)	0.0114(19)	0.005(2)	0.0352(10)
X^P_A	0.2525(10)	0.7336(8)	0.0083(5)	0.035(3)	0.063(3)	0.039(3)	0.015(2)	0.010(2)	0.004(2)	0.0454(12)
H1	0.378(13)	0.300(9)	−0.007(5)	0.04225*						
H2	0.208(10)	0.466(4)	0.017(5)	0.04225*						
H3	0.20210(0)	0.64860(0)	−0.0612(12)	0.05443*						
H4	0.353(13)	0.655(5)	0.070(3)	0.05443*						

*U_{iso}

Table 5. Selected interatomic distances (Å) and angles (°) in MRM.

M^O1–X^O_A	1.907(3)	M^O2–O6(d)	2.239(5)	Si1–O2	1.593(4)	Si2–O5	1.583(4)
M^O1–X^O_A(a)	1.913(4)	M^O2–X^O_M(a)	2.359(5)	Si1–O1(d)	1.595(4)	Si2–O7(d)	1.588(4)
M^O1–X^O_A(b)	2.013(4)	M^O2–O6(a)	2.402(5)	Si1–O3(a)	1.637(4)	Si2–O6(d)	1.622(4)
M^O1–O6	2.015(4)	M^O2–X^O_A	2.440(5)	Si1–O4(e)	1.638(4)	Si2–O4	1.628(4)
M^O1–O3	2.118(3)	M^O2–X^O_M	2.492(5)	<Si1–O>	1.616	<Si2–O>	1.605
M^O1–O3(c)	2.126(3)	M^O2–O3(d)	2.791(5)				
<M^O1–φ>	2.015	<M^O2–φ>	2.454				
M^H1–X^P_M	1.792(8)	M^H2–X^P_M	1.89(4)	A^P–X^P_A	2.306(6)	Si1(f)–O4–Si2	138.1(3)
M^H1–O7	1.921(4)	M^H2–O7	1.90(1)	A^P–X^O_A	2.478(4)	Short distances	
M^H1–O5	1.930(4)	M^H2–O5	1.93(1)	A^P–O12(f)	2.529(5)	M^H1–M^H2	0.38(3)
M^H1–O11	1.937(4)	M^H2–O1	1.94(1)	A^P–O1(f)	2.558(5)		
M^H1–O12	1.956(4)	M^H2–O12	1.95(1)	A^P–O7	2.577(6)		
M^H1–X^P_M	2.267(8)	M^H2–X^O_M	2.17(4)	A^P–O5	2.634(6)		
<M^H1–φ>	1.967	<M^H2–φ>	1.96	A^P–O4(g)	2.670(5)		
				A^P–O4	2.709(5)		
				<A^P–φ>	2.558		

φ = O, F, OH, H_2O;
Symmetry operators (given in brackets): a: −x + 1, −y + 1, −z + 1; b: −x + 1, −y + 2, −z + 1; c: −x, −y + 2, −z + 1; d: x + 1, y, z; e: x, y − 1, z; f: x, y + 1, z; g: x − 1, y, z.

Table 6. Refined site-scattering values and assigned site-populations for MRM.

Site*	Refined site-scattering (epfu)	Assigned site population (pfu)	Calculated site-scattering (epfu)	<cation–φ>$_{obs.}$ (Å)	Ideal composition (pfu)
Cations					
M^H1	42(1)	Ti$_{1.88}$Al$_{0.01}$□$_{0.11}$	41.49	1.967	
M^H2	5(1)	Nb$_{0.11}$□$_{1.89}$	4.51	1.96	
M^H	47	Ti$_{1.88}$Nb$_{0.11}$Al$_{0.01}$	46.00		Ti$_2$
M^O1	46.2(3)	Ti$_{1.13}$Nb$_{0.28}$Mn$_{0.20}$Fe$^{2+}_{0.19}$Mg$_{0.17}$Zr$_{0.01}$□$_{0.02}$	48.72	2.015	Ti$_2$
M^O2	16.3(12)	Ca$_{0.63}$Na$_{0.42}$□$_{0.95}$	17.22	2.454	(Ca□)
$^{[8]}A^P$	24.8(1)	Na$_{1.70}$Ca$_{0.22}$K$_{0.07}$Sr$_{0.01}$	24.81	2.558	Na$_2$
Anions** and H_2O groups					
X^O_M		O$_{2.00}$			O$_2$
X^O_A		O$_{1.90}$F$_{0.10}$			O$_2$
Σ		O$_{3.90}$F$_{0.10}$			O$_4$
$^{[1]}X^P_M$		(H_2O)$_{1.89}$(OH)$_{0.11}$			(H_2O)$_2$
$^{[1]}X^P_A$		(H_2O)$_2$			(H_2O)$_2$
Σ		(H_2O)$_{3.89}$(OH)$_{0.11}$			(H_2O)$_4$

*Coordination numbers are shown for non-[6]-coordinated cation sites and non-[4]-coordinated anion sites and H_2O groups; φ = O, F, OH, H_2O.
**Anions which do not coordinate Si.

Table 7. Bond-valence values (vu)* for MRM.

Atom Occupancy %	M^O1 100	M^O2 53	M^H1 95	M^H2 5	A^P 100	Si1 100	Si2 100	H1 100	H2 100	H3 100	H4 100	Σ
O1			0.66	0.05	0.14	1.07						1.92
O2			0.63	0.04	0.15	1.08						1.90
O3	0.44	0.06				0.96						1.89
	0.43											
O4					0.12	0.96	0.98					2.06
$^{[3]}$O5			0.63	0.05	0.11		1.11				0.06	1.96
O6	0.57	0.17					1.00					1.87
		0.13										
$^{[3]}$O7			0.69	0.05	0.14		1.10			0.06		2.04
X_M^O	0.74	0.14	0.99	0.03								2.01
		0.11										
X_A^O	0.75	0.13			0.16							1.67
	0.57											
$^{[1]}X_M^P$			0.29	0.05				0.86	0.85		0.09	2.14
$^{[1]}X_A^P$				0.22				0.14	0.15	0.94	0.85	2.30
Total	3.50	0.74	3.93	0.27	1.16	4.07	4.19	1.00	1.00	1.00	1.00	
Aggregate charge	3.54	0.84	3.80	0.25	1.12	4.00	4.00					

*Bond-valence parameters (vu) are from Brown (1981) and Brown and Altermatt (1985) for hydrogen bonding; for O atoms, coordination numbers [ ] are given where an O atom is coordinated by less than four cations; bond-valence values are calculated with cation–O parameters for: $M^O1 = Ti$; $M^O2 = Ca_{0.60}Na_{0.40}$; $M^H1 = Ti$; $M^H2 = Nb$ and $A^P = Na$.

Table 8. Hydrogen bonding in MRM.

D–H···A	D–H (Å)	H···A (Å)	D···A (Å)	∠DHA (°)
X_M^P–H1···X_A^P(a)	0.98(1)	2.00(5)	2.83(7)	140(6)
X_M^P–H2···X_A^P	0.98(1)	1.91(3)	2.802(7)	149(5)
X_A^P–H3···O7(b)	0.98(1)	2.63(3)	3.516(7)	149.9(5)
X_A^P–H4···X_M^P	0.98(1)	2.21(4)	2.802(7)	117(3)
X_A^P–H4···O5	0.98(1)	2.46(12)	3.420(7)	167(4)

Symmetry operators (in brackets): a: $-x+1, -y+1, -z$; b: $-x, -y+1, -z$.

Site-population assignment

Ti-dominant sites

In the seidozerite-supergroup minerals, Ti-dominant sites are always fully occupied (Sokolova, 2006; Sokolova and Cámara, 2017). In the murmanite-group minerals, Ti = 4 apfu; in the O sheet, Ti = 2 apfu (Fig. 1a) and Ti-dominant sites in the O sheet commonly contain divalent cations such as Mn, Fe^{2+} and Mg (Sokolova, 2006; Sokolova and Cámara, 2017); in the H sheet, Ti = 2 apfu (Fig. 1b). In MRM, the $^{[6]}M^H$ site in the H sheet, which gives 2 apfu, splits into two subsites, M^H1 and M^H2, with refined site-scattering values of 42(1) and 5(1) electrons per formula units (epfu) and mean bond-lengths of 1.967 and 1.96 Å, respectively (Table 6). The short distance of 0.38 Å between the two subsites indicates that these subsites can be only alternately occupied. Total refined site-scattering for the M^H site is 47 epfu (more than the 44 epfu corresponding to occupancy by Ti_2 apfu) and hence the M^H site must be occupied by Ti plus a heavier cation, e.g. Nb, Zr, Mn and Fe^{2+}, available from the chemical analysis (Table 2). The calculated cation radius (r) for the M^H2 site is 1.96–1.38 ($^{[4]}O^{2-}$, Shannon, 1976) = 0.58 Å. The $^{[6]}Nb$ has the smallest ionic radius (0.64 Å) compared to Zr (0.72 Å), Mn (0.83 Å) and Fe^{2+} (0.78 Å). We assign the rest of Ti and Nb available from the chemical analysis (Table 2) plus all Zr, Mn, Fe^{2+} and Mg to the M^O1 site in the O sheet: $Ti_{1.13}Nb_{0.28}Mn_{0.20}Fe^{2+}_{0.19}Mg_{0.17}Zr_{0.01}\square_{0.02}$ pfu, with close agreement between refined and calculated site-scattering values, 46.2 and 48.72 epfu, respectively (Table 6).

Alkaline and alkali-earth sites

Chemical analysis (Table 2) gives alkali and alkali-earth cations $(Na_{2.12}Ca_{0.85}K_{0.07}Sr_{0.01})_{\Sigma3.05}$ apfu to assign to the A^P and M^O2 sites, which give 4 apfu. The $^{[8]}A^P$ site in the H sheet of MRM has a refined site-scattering value of 24.8(1) epfu and a mean bond length of 2.558 Å (Fig. 1b, Table 6). In murmanite, the corresponding site is occupied by $Na_{1.78}Ca_{0.15}K_{0.05}\square_{0.02}$ pfu, ideally Na_2 apfu, and has a refined site-scattering value of 22.0(1) epfu and a mean bond length of 2.568 Å (Cámara et al., 2008). In the holotype calciomurmanite, (1) the corresponding site is occupied by $Ca_{1.16}\square_{0.84}$ pfu, with a refined site-scattering value of 23.2 epfu and a mean bond length of 2.553 Å; (2) the two additional [7] and [8]-coordinated sites between TS blocks are occupied by $Sr_{0.18}\square_{1.82}$ and $K_{0.10}\square_{1.90}$ pfu with refined site-scattering values of 7.0 and 2.0 epfu, respectively (Lykova et al., 2016). In the structures of murmanite (Cámara et al., 2008) and MRM, there are no additional sites between TS blocks; see Table 3 for the highest peak of 1.77 $e/Å^3$ in the difference Fourier map for MRM. To the largest $^{[8]}A^P$ site in MRM, we assign the largest alkaline and alkali-earth cations available from the chemical analysis (Table 2), $K_{0.07}Sr_{0.01}$ apfu ($^{[8]}K$: r = 1.51 Å; $^{[8]}Sr$: r = 1.26 Å), with the calculated site-scattering value of 1.71 epfu. We are left with the site-scattering value 24.8–1.71 = 23.09 epfu, which cannot be compensated by all available $Ca_{0.85}$ apfu, which has a calculated site-scattering value of 17 epfu. Hence we assign $Na_{1.70}Ca_{0.22}$ apfu ($^{[8]}Na$: r = 1.18 Å; $^{[8]}Ca$: r = 1.12 Å), with the calculated site-scattering value of 23.10 epfu. The $^{[8]}A^P$ site in MRM is occupied by $Na_{1.70}Ca_{0.22}K_{0.07}Sr_{0.01}$ apfu (Table 6).

The M^O2 site in the O sheet of MRM (Fig. 1a), has a refined site-scattering value of 16.3 epfu and a mean bond length of 2.454 Å. To the M^O2 site, we assign the remaining Ca and Na, $Ca_{0.63}Na_{0.42}\square_{0.95}$ pfu, where Ca > Na. The refined and calculated site-scattering values for the M^O2 site of 16.3 and 17.22 epfu, respectively, are in good agreement.

Description of the structure

Cation and anion sites

Here we consider six cation sites in the crystal structure of MRM: the M^H, A^P and two Si sites of the H sheet and the two M^O sites of
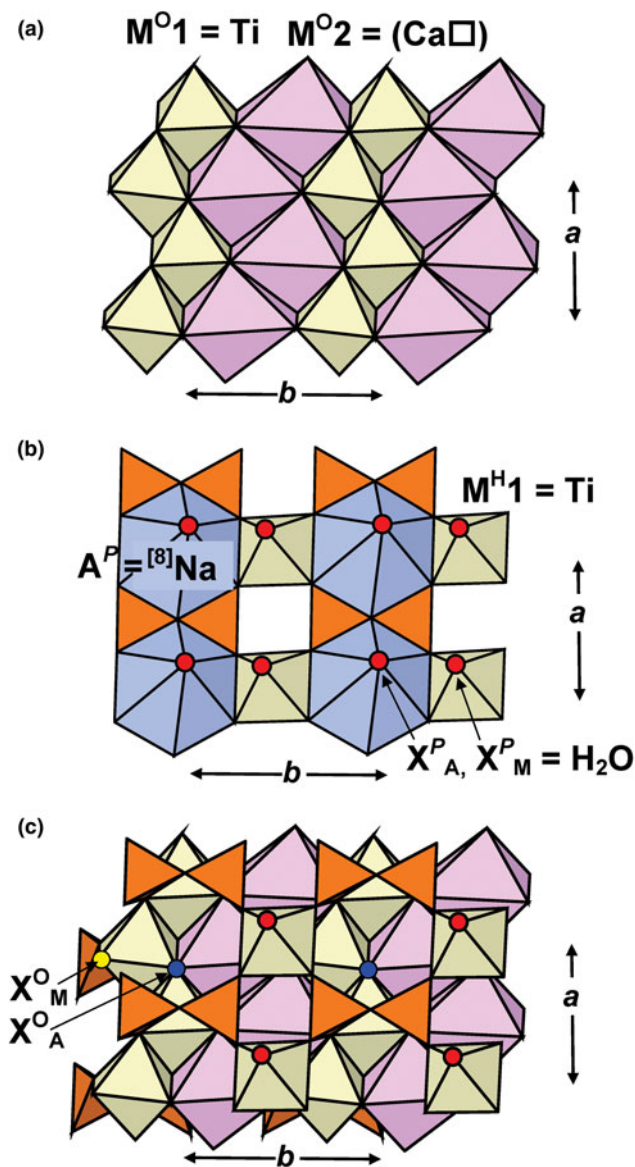
Fig. 1. Details of the TS block in MRM: the O sheet of Ti-dominant M^O1 and Ca-dominant M^O2 octahedra [M^O2 sites are occupied at 53%] (a); the H sheet of Si_2O_7 groups, Ti-dominant M^H octahedra and Na-dominant A^P polyhedra (b); the TS block (c). Si tetrahedra are orange, Ti-dominant octahedra are yellow; Na-dominant and Ca-dominant polyhedra are navy blue and pale pink, H_2O groups at the X^P sites are shown as large red spheres, X_M^O and X_A^O anions are shown as yellow and dark blue spheres in (c).

the O sheet; and six anion sites: X_M^O and X_A^O = anion sites at the common vertices of $3M^O$ and M^H polyhedra and $3M^O$ and A^P polyhedra, respectively; two $X_{(M,A)}^P$ = anion sites at the apical vertices of M^H octahedron and one $^{[8]}A^P$ polyhedron at the periphery of the TS block; labelling is in accord with Sokolova (2006). The specification of anions will be given at the end of this section.

In the O sheet, the Ti-dominant M^O1 site is coordinated by four O atoms and two X_A^O anions of the following composition $(O_{0.95}F_{0.05})$, with $< M^O1-\varphi> = 2.015$ Å (φ = unspecified anion) (Tables 5,6; Figs 1a,c). The ideal composition of the M^O1 site is Ti_2 apfu (Table 6). In murmanite, the Ti-dominant site is coordinated by six O atoms. The M^O2 site is 53% occupied by Ca and Na (Ca > Na) (Table 6, Fig. 1a), and is coordinated by five O atoms and an X_A^O anion, with $< M^O2-\varphi> = 2.454$ Å (Table 5).

The ideal composition of the M^O2 site is (Ca☐) pfu (Table 6). In murmanite, the corresponding site is occupied by $Na_{1.55}Mn_{0.14}Ca_{0.06}☐_{0.25}$ pfu, ideally Na_2 apfu, with a mean bond length of 2.468 Å (Cámara et al., 2008). In holotype and cotype calciomurmanite, the corresponding site is occupied by $Na_{1.42}☐_{0.58}$ and $Na_{1.02}☐_{0.98}$ pfu, respectively, ideally (Na☐) pfu, with mean bond lengths of 2.454 and 2.467 Å, respectively (Lykova et al., 2016). Note that for the holotype calciomurmanite, the chemical analysis gives only 1.34 Na apfu [Table 2, analysis (3)]. The ideal composition of the $M^O2 + M^O1$ sites is (Ca☐)Ti_2 apfu.

In the H sheet, there are two tetrahedrally coordinated sites ($Si1$, $Si2$) occupied by Si. There is one Ti-dominant $^{[6]}M^H$ site which splits into two subsites; each $M^H1,2$ subsite is coordinated by five O atoms and an H_2O group or an OH group at the X_M^P site, with $< M^H1,2-\varphi> = 1.967$ and 1.96 Å (Figs 1b,c), respectively. The M^H1 and M^H2 subsites are 0.38 Å apart and they are occupied by $Nb_{0.11}☐_{1.89}$ and $Ti_{1.88}Al_{0.01}☐_{0.11}$ pfu, respectively (Table 6). Positional Ti–Nb disorder within one site has been reported for several Ti-silicates, e.g. in the O sheet of fogoite-(Y), ideally $Na_3Ca_2Y_2Ti(Si_2O_7)_2OF_3$ (Cámara et al., 2017), a rinkite-group mineral (seidozerite supergroup), and in the H sheet of veblenite, $K_2☐_2Na(Fe_5^{2+}Fe_4^{3+}Mn_7^{2+}☐)Nb_3Ti(Si_2O_7)_2(Si_8O_{22})_2O_6(OH)_{10}(H_2O)_3$ (Cámara et al., 2013b). The M^H site ideally gives Ti_2 apfu. The $^{[8]}A^P$ site is occupied mainly by Na, less Ca, and minor K and Sr, and is ideally Na_2 apfu (Table 6). The A^P site is coordinated by six O atoms, an (O,F) anion (O >> F) at the X_A^O site and an H_2O group at the X_A^P site, with $< A^P-\varphi> = 2.558$ Å (Figs 1b,c; Table 5). The ideal composition of the $A^P + M^H$ sites is Na_2Ti_2 apfu.

We write the cation part of the TS block as the sum of cations of the 2H and O sheets: ideally $Na_2Ti_2(Ca☐)Ti_2$ pfu, with a total charge of 20^+.

The two $Si1,2$ atoms and seven O(1–7) atoms that coordinate the Si atoms give $(Si_2O_7)_2$ pfu (Tables 4,5). An anion at the X_M^O site (Fig. 1c) receives bond valences from four cations: M^H1, M^H2, M^O2 and M^O1, with a total bond-valence sum of 2.01 vu (valence units) (Table 7); thus it is an O atom, giving O_2 apfu (Table 6). An anion at the X_A^O site (Fig. 1c) receives bond valences from four cations: $2(M^O1)$, M^O2 and A^P, with a total bond-valence sum of 1.67 vu (Table 7). We assign $O_{1.90}F_{0.10}$ to the X_A^O site, ideally $O_{2.00}$ apfu (Table 6). Joint occurrence of O and F atoms at the X_A^O site was reported for the murmanite-group minerals sobolevite, $Na_6(Na_2Ca)(NaCaMn)Na_2Ti_2Na_2(TiMn)(Si_2O_7)_2(PO_4)_4O_2(OF)F_2$ (Sokolova et al., 1988; Sokolova et al., 2005) and betalomonosovite, $Na_2☐_4Na_2Ti_2Na_2Ti_2(Si_2O_7)_2[PO_3(OH)][PO_2(OH)_2]O_2(OF)$ (Sokolova et al., 2015). The two $(X_{M,A}^O)_2$ sites ideally give O_4 apfu.

Consider the two $X_{(M,A)}^P$ sites at the periphery of the TS block (Figs 1c, 2). Figure 3 shows the general pattern of hydrogen bonding between H_2O groups at the $X_{(M,A)}^P$ sites of two adjacent TS blocks. Details of the hydrogen bonding are given in Table 8. This pattern is analogous to that in murmanite-group minerals: murmanite, originally proposed by Khalilov (1989) and described in detail (including positions of H atoms) by Cámara et al. (2008); in vigrishinite, $NaZnTi_4(Si_2O_7)_2O_3(OH)(H_2O)_4$ (Sokolova and Hawthorne, 2018); and in the lamprophyllite-group minerals: epistolite, $Na_4TiNb_2(Si_2O_7)_2O_2(OH)_2(H_2O)_4$ (Sokolova and Hawthorne, 2004) and zvyaginite, $Na_2ZnTiNb_2(Si_2O_7)_2O_2(OH)_2(H_2O)_4$ (Sokolova et al., 2017). In these structures, H_2O groups form a ribbon which extends along $\mathbf{a}$ ($\mathbf{t_1}$) (Fig. 3). The O atom of the H_2O group at the X_A^P site receives 0.22 vu from Na at the A^P site
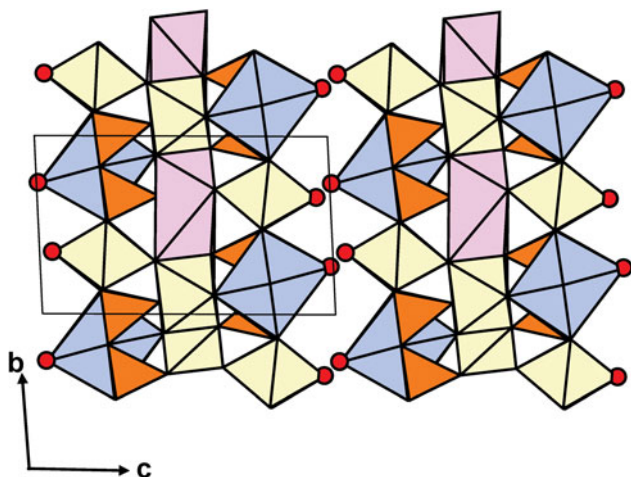
Fig. 2. A general view of the crystal structure of MRM. Legend as in Fig. 1.

Fig. 3. A general scheme of hydrogen bonding in MRM, only H_2O and OH groups are shown, O atoms involved in hydrogen bonding are omitted. O atoms of H_2O groups and OH groups at the X^P sites are shown as large and small red spheres, respectively; Na atoms at the A^P site are shown as navy blue spheres, and Ti and Nb atoms at the M^H1 and M^H2 subsites are shown as yellow spheres; Ti–O(H_2O), Nb–O(OH) and Na–O (H_2O) bonds are shown as solid black lines. D(donor)–A(acceptor) directions are shown as dashed lines.

(Table 7, Fig. 3) and we assign an H_2O group to the X^P_A site (Table 6). To assign species to the X^P_M site, we need to consider short-range order (SRO) arrangements involving the M^H1 and M^H2 subsites which are 95% occupied by Ti (and minor Al) and 5% occupied by Nb, respectively (Fig. 3). SRO-95% occurs where the M^H1 subsite is occupied by Ti and the M^H2 subsite is vacant, and the O atom at the X^P_M site receives bond valence only from one cation: 0.31 vu from Ti at the M^H1 subsite, with M^H1–O = 2.267 Å (Table 5). Hence at SRO-95%, the X^P_M site is occupied by H_2O groups (Fig. 3), giving 1.89 H_2O pfu (Table 6). SRO-5% occurs where the M^H1 is vacant and the M^H2 subsite is occupied by Nb, and the O atom at the X^P_M site receives bond valence only from one cation: 1.00 vu from Nb at the M^H2 subsite, with M^H2–O = 1.89 Å (Table 5). Hence at SRO-5%, the X^P_M site is occupied by OH groups (Fig. 3), giving 0.11 OH pfu (Table 6). In accord with the two SRO arrangements, SRO-95% and SRO-5%, we assign $(H_2O)_{1.89}(OH)_{0.11}$ pfu to the X^P_M site (Table 6). We sum the compositions of the two $X^P_{(M,A)}$ sites as follows: $(H_2O)_{1.89}(OH)_{0.11}$ pfu $[X^P_M]$ + $(H_2O)_{2.00}$ $[X^P_A]$ = $(H_2O)_{3.89}(OH)_{0.11}$, ideally $(H_2O)_4$ pfu (Table 6).

The anions and H_2O groups sum as follows: $(Si_2O_7)_2$ [O(1–7)] + O_2 $[X^O_M]$ + O_2 $[X^O_A]$ + $(H_2O)_4$ $[X^P_{(M,A)}]$ = $(Si_2O_7)_2O_4(H_2O)_4$ pfu, with a total charge of 20^-.

We write the ideal structural formula of MRM as the sum of cation and anion parts: $Na_2Ti_2(Ca\square)Ti_2$ + $(Si_2O_7)_2O_4(H_2O)_4$ = $Na_2Ti_2(Ca\square)Ti_2(Si_2O_7)_2O_4(H_2O)_4$ with $Z = 1$. A short form of the ideal structural formula is $Na_2CaTi_4(Si_2O_7)_2O_4(H_2O)_4$.

Structure topology of MRM

The crystal structure of the MRM is topologically identical to the structures of murmanite (Cámara *et al.*, 2008) and calciomurmanite (Lykova *et al.*, 2016) and is related to vigrishinite (Sokolova and Hawthorne, 2018). The main structural unit in the crystal structure of MRM is a TS block that consists of HOH sheets. In accord with Sokolova and Cámara (2013), it is a basic structure, structure type B1MG.

The O sheet is composed of Ti-dominant M^O1 octahedra and Ca-dominant M^O2 octahedra occupied at 53%; M^O1 and M^O2 octahedra each form brookite-like chains along **a** (Fig. 1*a*). Ideal compositions of the O sheet in MRM, calciomurmanite and
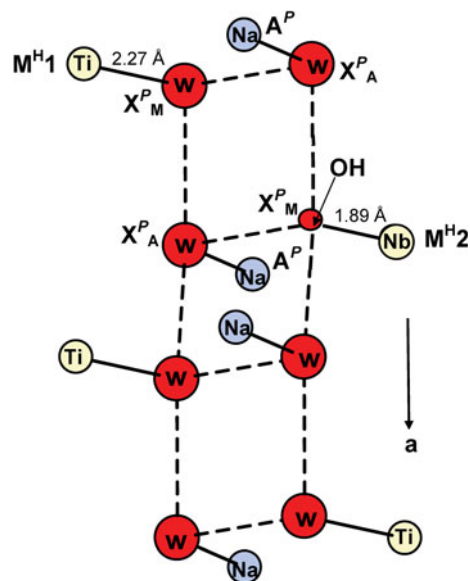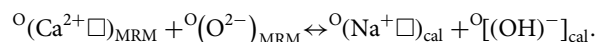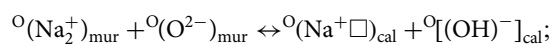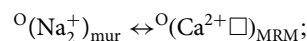
murmanite are $[(Ca\square)Ti_2O_4]^{2+}$ pfu, $[(Na\square)Ti_2O_3(OH)]^{2+}$ pfu and $[Na_2Ti_2O_4]^{2+}$ apfu, respectively.

Murmanite, MRM and calciomurmanite are related by the following substitutions in the O sheet:

$$^O(Na_2^+)_{mur} \leftrightarrow ^O(Ca^{2+}\square)_{MRM};$$

$$^O(Na_2^+)_{mur} + ^O(O^{2-})_{mur} \leftrightarrow ^O(Na^+\square)_{cal} + ^O[(OH)^-]_{cal};$$

$$^O(Ca^{2+}\square)_{MRM} + ^O(O^{2-})_{MRM} \leftrightarrow ^O(Na^+\square)_{cal} + ^O[(OH)^-]_{cal}.$$

In MRM, the H sheet is built of Si_2O_7 groups, Ti-dominant $^{[6]}M^H$ octahedra and Na-dominant $^{[8]}A^P$ polyhedra (Fig. 1*b*). Ideal compositions of the H sheets in MRM and murmanite are identical: $[Na_2Ti_2(Si_2O_7)_2(H_2O)_4]^{2-}$ apfu; ideal composition of the H sheets in calciomurmanite is $[Ca\square Ti_2(Si_2O_7)_2(H_2O)_4]^{2-}$ pfu. Murmanite + MRM and calciomurmanite are related by the following substitution in the H sheet:

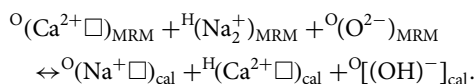$$^H(Na_2^+)_{mur,MRM} \leftrightarrow ^H(Ca^{2+}\square)_{cal}.$$
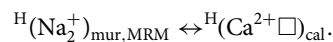
In MRM, the topology of the TS block is as in the murmanite group of TS-block minerals [Ti + Mg + Mn = 4 apfu]: Si_2O_7 groups link to two Ti octahedra of the O sheet adjacent along t_1 (Fig. 1*c*). In the crystal structure of MRM, TS blocks parallel to (001) link via hydrogen bonds between H_2O groups at apical vertices $[X^P_{(M,A)}$ sites] of M^H and A^P polyhedra (Fig. 2; for the pattern of hydrogen bonding, see Fig. 3).

MRM and murmanite are related by the following substitution:

$$^O(Ca^{2+}\square)_{MRM} \leftrightarrow ^O(Na_2^+)_{mur}.$$

MRM and calciomurmanite are related by the following substitution:

$$^O(Ca^{2+}\square)_{MRM} + {}^H(Na_2^+)_{MRM} + {}^O(O^{2-})_{MRM}$$

$$\leftrightarrow {}^O(Na^+\square)_{cal} + {}^H(Ca^{2+}\square)_{cal} + {}^O[(OH)^-]_{cal}.$$

We conclude that: (1) the general topology of the crystal structure of MRM described above is in accord with the topology of murmanite (Khalilov, 1989; Cámara *et al.*, 2008) and calciomurmanite (Lykova *et al.*, 2016); and (2) the stereochemistry of Ca and Na in the TS block is different from that reported for calciomurmanite (Lykova *et al.*, 2016): disorder of Ca and $\square$ in the O sheet of MRM versus disorder of Ca and $\square$ in the H sheet of calciomurmanite (Table 1). A similar stereochemistry of Zn and $\square$ was described for two TS-block minerals: the order of Zn and $\square$ in the O sheet of zvyaginite (Pekov *et al.*, 2014; Sokolova *et al.*, 2017) and the order of Zn and $\square$ in the H sheet of vigrishinite (Pekov *et al.*, 2013; Sokolova and Hawthorne, 2018).

Summary

Electron-microprobe analysis of MRM from the Mt. Pyalkimpor, Lovozero alkaline massif, Kola Peninsula, Russia, is in accord with that of 'calciomurmanite' from the Shcherbakovitovoe pegmatite, Mt. Koashva, Khibiny (Lykova *et al.*, 2016, Table 1, analysis 6). The empirical formula of MRM, $(Na_{2.12}K_{0.07}Sr_{0.01})_{\Sigma2.20}Ca_{0.85}$ $(Ti_{3.01}Nb_{0.39}Mn_{0.20}Fe^{2+}_{0.19}Mg_{0.17}Zr_{0.01}Al_{0.01})_{\Sigma3.98}(Si_{4.20}O_{14})[O_{3.90}$ $F_{0.10}]_{\Sigma4}[(H_2O)_{3.89}(OH)_{0.11}]_{\Sigma4}\{P_{0.03}\}$ with $Z = 1$, gives the sum of alkali and alkali-earth cations as 3.05 apfu and Na:Ca $\approx$ 2 : 1. The incomplete empirical formula of 'calciomurmanite' from the Shcherbakovitovoe pegmatite, Mt. Koashva, Khibiny [Lykova *et al.*, 2016, Table 1, analysis 6; this paper, Table 2, analysis (2)] gives a sum of alkali and alkali-earth cations, $(Na_{2.32}K_{0.11})_{\Sigma2.43}Ca_{1.00}$, with $\Sigma = 3.43$ apfu and Na:Ca $\approx$ 2:1. For the holotype calciomurmanite, alkali and alkali-earth cations are as follows $(Na_{1.34}K_{0.05})_{\Sigma1.39}Ca_{1.04}$, $\Sigma = 2.43$ apfu and Na:Ca $\approx$ 1:1.

The crystal structure of MRM has been refined in space group $P\bar{1}$, $a = 5.363(2)$, $b = 7.071(2)$, $c = 12.176(5)$ Å, $\alpha = 92.724(3)$, $\beta = 107.542(7)$, $\gamma = 90.13(2)°$, $V = 439.7(4)$ Å^3, $R_1 = 5.72\%$ and $Z = 1$. The general topology of the crystal structure of MRM is in accord with the topology of murmanite (Khalilov, 1989; Cámara *et al.*, 2008) and calciomurmanite (Lykova *et al.*, 2016): it is an array of TS blocks connected via hydrogen bonds between H$_2$O groups. However the stereochemistry of the TS block is different from that in the calciomurmanite of Lykova *et al.* (2016). In MRM, there is disorder of Ca and $\square$ at the M^O2 site in the O sheet of the composition $[(Ca\square)Ti_2O_4]^{2+}$. In calciomurmanite, there is disorder of Ca and $\square$ at the A^P site in the H sheets of the composition $[(Ca\square)Ti_2(Si_2O_7)_2(H_2O)_4]^{2-}$.

MRM has an ideal structural formula of the form $A_2^P M_2^H M_4^O (Si_2O_7)_2(X_M^O)_2(X_A^O)_2(X_{M,A}^P)_4$: $Na_2Ti_2(Ca\square)Ti_2(Si_2O_7)_2$ $O_4(H_2O)_4$, in a shorter form $Na_2CaTi_4(Si_2O_7)_2O_4(H_2O)_4$, $Z = 1$.

MRM is a Ca-rich and Na-poor analogue of murmanite, ideally $Na_2Ti_2Na_2Ti_2(Si_2O_7)_2O_2O_2(H_2O)_4$. MRM is a Na-rich and OH-poor analogue of calciomurmanite, ideally $(Ca\square)$ $Ti_2(Na\square)Ti_2(Si_2O_7)_2O_2[O(OH)](H_2O)_4$. MRM and (murmanite and calciomurmanite) are related by the following substitutions: $^O(Ca^{2+}\square)_{MRM} \leftrightarrow {}^O(Na_2^+)_{mur}$ and $^O(Ca^{2+}\square)_{MRM} + {}^H(Na_2^+)_{MRM}$ $+ {}^O(O^{2-})_{MRM} \leftrightarrow {}^O(Na^+\square)_{cal} + {}^H(Ca^{2+}\square)_{cal} + {}^O[(OH)^-]_{cal}.$

MRM is a possible new mineral of the murmanite group (seidozerite supergroup) where Ti + Mg + Mn = 4 apfu. We feel it is more appropriate that Inna Lykova proposes MRM as a new mineral as she found it in the field (personal communication, Dmitriy Belakovskiy), and because Lykova *et al.* (2016) reported a composition very similar to MRM from the Shcherbakovitovoe pegmatite, Mt. Koashva, Khibiny.

References

Brown I.D. (1981) The bond-valence method: an empirical approach to chemical structure and bonding. Pp. 1–30 in: *Structure and Bonding in Crystals II* (M. O'Keeffe and A. Navrotsky, editors). Academic Press, New York.

Brown I.D. and Altermatt D. (1985) Bond-valence parameters obtained from a systematic analysis of the inorganic crystal structure database. *Acta Crystallographica*, **B41**, 244–247.

Cámara F., Sokolova E., Hawthorne F.C. and Abdu Y. (2008) From structure topology to chemical composition. IX. Titanium silicates: revision of the crystal chemistry of lomonosovite and murmanite, Group-IV minerals. *Mineralogical Magazine*, **72**, 1207–1228.

Cámara F., Sokolova E. and Nieto F. (2009) Cámaraite, $Ba_3NaTi_4(Fe^{2+},Mn)_8$ $(Si_2O_7)_4O_4(OH,F)_7$. II. The crystal structure and crystal chemistry of a new group-II Ti-disilicate mineral. *Mineralogical Magazine*, **73**, 855–870.

Cámara F., Sokolova E., Abdu Y.A., Hawthorne F.C. and Khomyakov A.P. (2013a) Kolskyite, $(Ca\square)Na_2Ti_4(Si_2O_7)_2O_4(H_2O)_7$, a Group-IV Ti-disilicate mineral from the Khibiny alkaline massif, Kola Peninsula, Russia: description and crystal structure. *The Canadian Mineralogist*, **51**, 921–936.

Cámara F., Sokolova E., Hawthorne F.C., Rowe R., Grice J.D. and Tait K.T. (2013b) Veblenite, $K_2\square_2Na(Fe^{2+}_5Fe^{3+}_4Mn^{2+}_7\square)Nb_3Ti(Si_2O_7)_2(Si_8O_{22})_2O_6$ $(OH)_{10}(H_2O)_3$, a new mineral from Seal Lake, Newfoundland and Labrador: mineral description, crystal structure, and a new veblenite (Si_8O_{22}) ribbon. *Mineralogical Magazine*, **77**, 2955–2974.

Cámara F., Sokolova E., Abdu Y.A., Hawthorne F.C., Charrier T., Dorcet V. and Carpentier J.-F. (2017) Fogoite-(Y), $Na_3Ca_2Y_2Ti(Si_2O_7)_2OF_3$, a Group-I TS-block mineral from the Lagoa do Fogo, the Fogo volcano, the São Miguel Island, the Azores: Description and crystal structure. *Mineralogical Magazine*, **81**, 383–402.

Gutkova N. (1930) Sur un nouveau titano-silicate – la mourmanite de Lujawrurt. *Comptes Rendus de l'Académie des Sciences de l'URSS*, **27**, 731–736 [in Russian].

Khalilov A.D. (1989) Refinement of the crystal structure of murmanite and new data on its crystal chemistry properties. *Mineralogicheskii Zhurnal*, **11**, 19–27 [in Russian].

Lykova I.S., Pekov I.V., Chukanov N.V., Belakovskiy D.I., Yapaskurt V.O., Zubkova N.V., Britvin S.N. and Giester G. (2015) Calciomurmanite, IMA 2014-103.CNMNC Newsletter No. 25, June 2015, page 530; *Mineralogical Magazine*, **79**, 529–535.

Lykova I.S., Pekov I.V., Chukanov N.V., Belakovskiy D.I., Yapaskurt V.O., Zubkova N.V., Britvin S.N. and Giester G. (2016) Calciomurmanite, $(Na,\square)_2Ca(Ti,Mg,Nb)_4[Si_2O_7]_2$ $O_2(OH,O)_2(H_2O)_4$, a new mineral from the Lovozero and Khibiny alkaline compexes, Kola Peninsula, Russia. *European Journal of Mineralogy*, **28**, 835–845.

Pekov I.V., Britvin S.N., Zubkova N.V., Chukanov N.V., Bryzgalov I.A., Lykova I.S., Belakovskiy D.I. and Pushcharovsky D.Yu. (2013) Vigrishinite, Zn_2Ti_{4-x} $Si_4O_{14}(OH,H_2O,\square)_8$, a new mineral from the Lovozero alkaline complex, Kola Peninsula, Russia. *Geology of Ore Deposits*, **55**, 575–586.

Pekov I.V., Lykova I.S., Chukanov N.V., Yapaskurt V.O., Belakovskiy D.I., Zolotarev Jr. A.A. and Zubkova N.V. (2014) Zvyaginite, NaZnNb$_2$Ti (Si$_2$O$_7$)$_2$O(OH,F)$_3$(H$_2$O)$_{4+x}$ (x < 1), a new mineral of the epistolite group from the Lovozero alkaline pluton, Kola Peninsula, Russia. *Geology of Ore Deposits*, **56**, 644–656.

Pouchou J.L. and Pichoir F. (1985) "PAP" φ(ρZ) procedure for improved quantitative microanalysis. Pp. 104–106 in: *Microbeam Analysis* (J.T. Armstrong, editor). San Francisco Press, San Francisco, California, USA.

Shannon R.D. (1976) Revised effective ionic radii and systematic studies of interatomic distances in halides and chalcogenides. *Acta Crystallographica*, **A32**, 751–767.

Sheldrick G.M. (2008) A short history of SHELX. *Acta Crystallographica*, **A64**, 112–122.

Sheldrick G.M. (2015) Crystal structure refinement with *SHELXL*. *Acta Crystallographica*, **C71**, 3–8.

Sokolova E. (2006) From structure topology to chemical composition. I. Structural hierarchy and stereochemistry in titanium disilicate minerals. *The Canadian Mineralogist*, **44**, 1273–1330.

Sokolova E. and Cámara F. (2013) From structure topology to chemical composition. XVI. New developments in the crystal chemistry and prediction of new structure topologies for titanium disilicate minerals with the TS block. *The Canadian Mineralogist*, **51**, 861–891.

Sokolova E. and Cámara F. (2017) The seidozerite supergroup of TS-block minerals: nomenclature and classification, with change of the following names: rinkite to rinkite-(Ce), mosandrite to mosandrite-(Ce), hainite to hainite-(Y) and innelite-1T to innelite-1A. *Mineralogical Magazine*, **81**, 1457–1484.

Sokolova E. and Hawthorne F.C. (2004) The crystal chemistry of epistolite. *The Canadian Mineralogist*, **42**, 797–806.

Sokolova E. and Hawthorne F.C. (2018) From structure topology to chemical composition. XXIV. Revision of the crystal structure and chemical formula of vigrishinite, NaZnTi$_4$(Si$_2$O$_7$)$_2$O$_3$(OH)(H$_2$O)$_4$, a seidozerite-supergroup mineral from the Lovozero alkaline massif, Kola peninsula, Russia. *Mineralogical Magazine*, **82**, 787–807.

Sokolova E.V., Egorov-Tismenko Yu.K. and Khomyakov A.P. (1988) Crystal structure of sobolevite. *Soviet Physics Doklady*, **33**, 711–714.

Sokolova E., Hawthorne F.C. and Khomyakov A.P. (2005) Polyphite and sobolevite: revision of their crystal structures. *The Canadian Mineralogist*, **43**, 1527–1544.

Sokolova E., Abdu Y.A., Hawthorne F.C., Genovese A., Cámara F. and Khomyakov A.P. (2015) From structure topology to chemical composition. XVIII. Titanium silicates: revision of the crystal structure and chemical formula of betalomonosovite, a Group-IV TS-block mineral from the Lovozero alkaline massif, Kola Peninsula, Russia. *The Canadian Mineralogist*, **53**, 401–428.

Sokolova E., Genovese A., Falqui A., Hawthorne F.C. and Cámara F. (2017) From structure topology to chemical composition. XXIII. Revision of the crystal structure and chemical formula of zvyaginite, Na$_2$ZnTiNb$_2$(Si$_2$O$_7$)$_2$O$_2$(OH)$_2$(H$_2$O)$_4$, a seidozerite-supergroup mineral from the Lovozero alkaline massif, Kola peninsula, Russia. *Mineralogical Magazine*, **81**, 1533–1550.

Wilson A.J.C. (editor) (1992) *International Tables for Crystallography. Volume C: Mathematical, physical and chemical tables*. Kluwer Academic Publishers, Dordrecht, The Netherlands.